

Preparation and Physico-chemical Properties of the Ternary Complexes formed between Adenosine 5'-Triphosphoric Acid, Bis(2-pyridyl)amine, and Divalent Metal Ions. Crystal and Molecular Structures of the Compounds containing Mg^{II} and Ca^{II} †

Renzo Cini *

Istituto di Chimica Generale della Università di Siene, Pian dei Mantellini 44, 53100 Siene, Italy

Maria C. Burla, Antonio Nunzi, Gian P. Polidori, and Pier F. Zanazzi

Istituto di Mineralogia della Università di Perugia, Piazza della Università, 06100 Perugia, Italy

Ternary compounds formed between M (Mg^{II}, Ca^{II}, Sr^{II}, Mn^{II}, Co^{II}, Cu^{II}, or Zn^{II}), adenosine 5'-triphosphate [adenosine 5'-triphosphate(4-) = atp], and bis(2-pyridyl)amine (bipyam) have been prepared. The solid compounds are crystalline and have a stoichiometry described by the formula M(Hatp)(Hbipyam)·nH₂O (n = 2–9). X-Ray powder diffraction patterns are similar. Potentiometric titrations in aqueous solution show the presence of two ionizable protons. Visible spectra suggest an octahedral co-ordination geometry. I.r. spectra indicated essentially the same type of metal–ligand interactions in all the complexes and show that Hatp³⁻ co-ordinates to the metal through the oxygen atoms of the α, β, and γ phosphate groups. The ternary compounds where M = Mg^{II} (1) or Ca^{II} (2) have been studied by single-crystal X-ray diffraction techniques and their molecular structures determined. The two species are isostructural and can be formulated as [Mg(H₂O)₆][Hbipyam]₂[Mg(Hatp)₂]·12H₂O (1) and [Ca(H₂O)₆][Hbipyam]₂[Ca(Hatp)₂]·9H₂O (2). Both (1) and (2) crystallise in space group C222₁ (Z = 4), with a = 22.734(3), b = 10.233(3), c = 30.997(4) Å for (1) and a = 22.965(3), b = 10.154(3), c = 32.390(4) Å for (2). X-Ray diffraction data were collected on a Philips automatic diffractometer and the structures solved by direct methods using the SIR (Semi-invariant Representation) package and refined by full-matrix least squares to final R values of 0.111 and 0.124 (1 088 and 1 008 independent observed reflections) for (1) and (2) respectively. In the [M(Hatp)₂]⁴⁻ units the metal ions lie on a two-fold axis with an octahedral co-ordination geometry completed by the oxygen atoms of the α, β, and γ phosphate groups of two symmetry-related Hatp³⁻ molecules. The co-ordination polyhedron of (1) is nearly regular but in (2) it is significantly distorted. The phosphate chains have a folded configuration in both (1) and (2). In both complexes there are no bonding interactions between the metal ions and the adenine base. The metal atoms of the [M(H₂O)₆]²⁺ cations are also located on two-fold axes while the six co-ordinated water molecules form hydrogen bonds with the phosphate chains. The Hbipyam⁺ molecules do not co-ordinate to the metal ions and are disordered around two-fold axes. Strong stacking interactions exist between Hbipyam⁺ and purine rings.

Nucleotides are involved in many fundamental processes of life. Most enzymes acting on these species need metal ions for their activity. Many investigations have shown that metal ion–nucleotide complexes are often the true substrate during enzymatic catalysis.^{1,2}

Interest in metal ion–nucleotide interactions has increased greatly since the discovery of antineoplastic complexes such as *cis*-[Pt(NH₃)₂Cl₂]. The anticancer activity of these drugs is believed to be due to the bond formation between the metal centre and the nucleotides in the nucleic acids.³ The metal ions can interact with different nucleotide donors such as the ribose or phosphate oxygen atoms and the nitrogen atoms of the base.

To understand the very important role of metal ions in biological processes involving nucleic acids and their fragments it is necessary to determine the nature of the possible interactions between the nucleotide donor centres and suitable metal cations. To this end in the last decade many studies have been carried out on different model complexes in aqueous solution and in the solid state.^{4,5}

In a recent paper the preparation and physico-chemical properties of a series of 1 : 1 : 1 ternary complexes involving adenosine-5'-triphosphate [adenosine 5'-triphosphate(4-) = atp], 2,2'-bipyridyl (bipy), and the metal ions Mn^{II}, Co^{II}, Cu^{II},

and Zn^{II} were reported.⁶ The crystal and molecular structure of the zinc derivative has also been determined.⁷

The present work deals with the preparation and characterization of a new series of ternary complexes involving atp, bis(2-pyridyl)amine (bipyam), and the divalent metal ions Mg^{II}, Ca^{II}, Sr^{II}, Mn^{II}, Co^{II}, Cu^{II}, Zn^{II} and includes the crystal and molecular structure determinations of the species containing magnesium and calcium. The structures of the Mn^{II} and Co^{II} derivatives will be reported elsewhere.⁸ Preliminary short notes on this series have also appeared.^{9–11} It has to be noted that for the first time a complex between atp and Mg^{II} has been isolated as a crystalline product and its molecular structure determined.

Experimental

Syntheses of the Ternary Complexes.—The disodium salt of adenosine-5'-triphosphoric acid, Na₂(H₂atp), was purchased from Sigma (St Louis) and used without further purification. Bis(2-pyridyl)amine (Analytical Grade) was purchased from Fluka and recrystallized from ethanol. Magnesium(II), calcium(II), strontium(II), manganese(II), cobalt(II), copper(II), and zinc(II) sulphates or nitrates were obtained from C. Erba (Milan). The salts were purified by crystallization from aqueous solutions. All other materials were reagent grade purchased from Merck.

General method. A solution of bipyam (1 × 10⁻³ mol) in 96% ethanol (5 cm³) was added to an aqueous solution (20

† Supplementary data available (No. SUP 56004, 18 pp.): structure factors, thermal parameters, See Instructions for Authors, *J. Chem. Soc., Dalton Trans.*, 1984, Issue 1, pp. xvii–xix.

Table 1. Elemental analysis for the ternary complexes *

Complex	Colour	C%	H%	N%	M%
(1) Mg(Hatp)(Hbipyam)·xH ₂ O	White	28.25 (27.85)	4.30 (4.80)	12.80 (13.00)	2.75 (2.80)
(2) Ca(Hatp)(Hbipyam)·xH ₂ O	White	28.50 (28.20)	4.60 (4.50)	12.60 (13.15)	4.50 (4.70)
(3) Sr(Hatp)(Hbipyam)·xH ₂ O	White	28.75 (28.75)	3.45 (3.75)	13.45 (13.40)	10.30 (10.50)
(4) Mn(Hatp)(Hbipyam)·xH ₂ O	White	28.00 (27.30)	4.45 (4.80)	13.35 (12.75)	6.65 (6.25)
(5) Co(Hatp)(Hbipyam)·xH ₂ O	Pale pink	27.75 (27.25)	4.50 (4.80)	13.45 (12.70)	7.05 (6.70)
(6) Cu(Hatp)(Hbipyam)·xH ₂ O	Green	30.70 (30.95)	3.30 (3.50)	14.70 (14.45)	8.40 (8.20)
(7) Zn(Hatp)(Hbipyam)·xH ₂ O	White	30.65 (30.90)	3.25 (3.50)	14.80 (14.40)	8.85 (8.40)

* The theoretical values (in parentheses) were calculated on the basis of $x = 9$ for (1), (4), and (5); 7.5 for (2), 4 for (3), and 2 for (6) and (7).

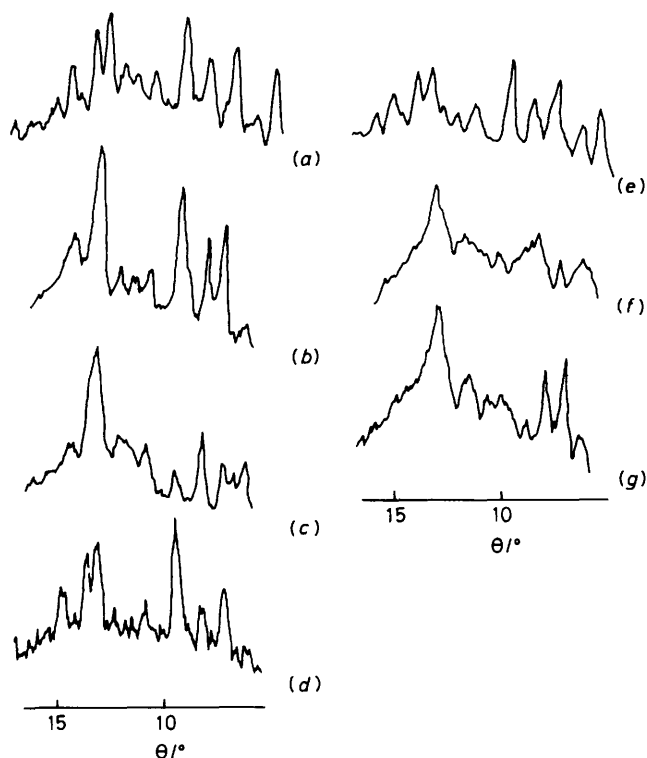


Figure 1. X-Ray powder diffraction diagrams of the M(Hatp)-(Hbipyam) complexes (1)–(7) obtained using Cu- K_{α} radiation monochromatized with a nickel filter: M = (a) Mg (1), (b) Ca (2), (c) Sr (3), (d) Mn (4), (e) Co (5), (f) Cu (6), and (g) Zn (7)

cm³) of Na₂(H₂atp) (1×10^{-3} mol). The resulting mixture was added to a solution (10 cm³) of the metal ion (1×10^{-3} mol). The final solution was heated to 80 °C for 10 min. The ternary complex precipitated upon cooling to room temperature, was collected by suction filtration, and washed three times with cold water and three times with ethanol. The product was recrystallized twice from water and then dried and conserved over silica gel.

The analytical data (C, H, N, and metal) for the ternary complexes are reported in Table 1. The compounds are microcrystalline and give similar X-ray powder diffraction patterns as shown in Figure 1. The yield of the purified complexes was ca. 60%.

Single crystals of the species containing Mg^{II}, Ca^{II}, Mn^{II}, and Co^{II} can be obtained by slow cooling of hot aqueous solutions. The small colourless needles of the Mg^{II} and Ca^{II} complexes and the pink prisms of the Co^{II} compound showed large mechanical deformities. This affected the accuracy of

Table 2. Crystal data for [Mg(H₂O)₆][Hbipyam]₂[Mg(Hatp)₂]₂·12H₂O (1) and [Ca(H₂O)₆][Hbipyam]₂[Ca(Hatp)₂]₂·9H₂O (2)

Formula	(1)	(2)
	C ₄₀ H ₈₂ Mg ₂ N ₁₆ O ₄₄ P ₆	C ₄₀ H ₇₆ Ca ₂ N ₁₆ O ₄₁ P ₆
<i>a</i> /Å	22.734(3)	22.965(3)
<i>b</i> /Å	10.233(3)	10.154(3)
<i>c</i> /Å	30.997(4)	32.390(4)
<i>U</i> /Å ³	7 211	7 553
<i>Z</i>	4	4
Space group	C222 ₁	C222 ₁
μ (Mo- K_{α})/cm ⁻¹	2.3	3.3
<i>M</i>	1 725.8	1 705.2
<i>D_c</i> /g cm ⁻³	1.59	1.50
<i>F</i> (000)	3 600	3 544
<i>R</i>	0.111	0.124
<i>R'</i>	0.110	0.127
Number of measured reflections	2 769	2 682
Number of observed reflections	1 088	1 008

the structure determinations. For the manganese compound relatively well shaped and larger crystals were obtained.

Apparatus.—Visible absorption spectra were recorded with a model 220 Perkin-Elmer spectrophotometer connected to a model 56 recorder. Reflectance spectra were measured on powdered samples with a Beckman DK2 spectrophotometer. Infrared spectra were recorded with Perkin-Elmer grating spectrophotometers (models 225 and 597) using Nujol mull and KBr pellets.

The pH measurements were obtained using a Metrohm digital potentiometer (model E603) with EA147 microglass electrodes. Potentiometric titrations were performed under nitrogen at 22 °C within Metrohm glass cells EA876 for initial volumes of 20 cm³. Aqueous solutions (1×10^{-3} mol dm⁻³) of the complexes or of the atp-bipyam mixture were prepared by weighing the calculated amounts of solids. The solutions were titrated with 0.0100 mol dm⁻³ NaOH. Carbon, H, and N analyses were performed with an elemental analyser, model 1102 C (Erba). Metal analyses were obtained by atomic absorption spectroscopy with a model 5000 Perkin-Elmer spectrometer using multielement Perkin-Elmer lamps and an acetylene-air flame.

Collection of X-Ray Data.—Well shaped crystals measuring ca. 0.15 × 0.10 × 0.05 mm and 0.20 × 0.10 × 0.08 mm were selected for (1) and (2) respectively and used for data collection on a Philips PW 1100 automatic diffractometer. Lattice constants were determined by the least-squares method applied to the setting angles of 25 reflections. Unit-cell parameters and other crystal data are reported in Table 2. Both crystals were found to belong to the orthorhombic system. We must note the similarities in the crystal data and

Table 3. Starting set used for the solution of complex (1). All nine one-phase semi-invariants were correctly determined

Origin fixing reflections					
<i>h</i>	<i>k</i>	<i>l</i>	Φ	<i>E</i>	
1	3	0	360	1.70	
0	2	23	360	2.73	
Symbols					
<i>h</i>	<i>k</i>	<i>l</i>	<i>E</i>		
11	3	22	2.65		
19	1	2	2.41		
0	2	13	2.59		
One-phase semi-invariants					
<i>h</i>	<i>k</i>	<i>l</i>	<i>E</i>	Estimated phase	Probability
16	0	14	2.77	360	1.0
0	2	22	1.87	180	1.0
0	6	0	2.77	180	1.0
0	4	20	2.08	360	1.0
12	0	0	1.61	180	1.0
0	0	6	1.78	180	1.0
0	6	6	1.44	360	1.0
0	4	14	1.72	180	1.0
16	0	0	1.86	180	1.0

intensity measurements of (1) and (2). In fact (1) and (2) are shown to be isostructural.

Systematic absences indicated the acentric space group $C222_1$, in accordance with the presence of an optically active ribose ring. Intensity data were collected in the range $4 \leq 2\theta \leq 40^\circ$ at $20 \pm 1^\circ\text{C}$ using Mo- K_α radiation ($\lambda = 0.71069 \text{ \AA}$) monochromatized with a graphite crystal. The θ - 2θ scan method was employed with a scan width of 1.40° in θ and a scan speed of $0.03^\circ \text{ s}^{-1}$. The intensity of three standard reflections was measured every 180 min to check the experimental conditions: no significant variation was detected during data collection. Totals of 1088 and 1008 reflections with $I > 3\sigma(I)$ were considered 'observed' and used for the structure solution and refinement for (1) and (2) respectively. Owing to the poor quality of the crystals many of the collected reflections were unobserved. In order to obtain the best data several measurements were carried out on different crystals and the refinement of the atomic positions carried out on the set with the highest number of observed reflections. The intensities were corrected for Lorentz-polarization effects; no absorption correction was applied.

Structure Solution and Refinement.—Several attempts to solve the structures using the Patterson method and the direct methods of MULTAN 80¹² and SHELX 76¹³ packages were unsuccessful. The structure of (1) was solved by using the SIR¹⁴ (Semi-invariant Representation) package utilizing three symbols and nine one-phase semi-invariants as known phases in the starting set. Of great help in the solution was the critical analysis of the convergence map and the check of the triplet relationships (T) of the type $T = SS1 + SS2$ against the separate estimates of one-phase semi-invariants (SS1)¹⁵ and special two-phase semi-invariants (SS2).¹⁶ The starting set is listed in Table 3. The *F* map computed with 357 reflections having $F > 1.4$ revealed all the metal atoms and all the non-hydrogen atoms of the Hatp³⁺ molecules.

The structure of (2) was solved starting from the partial model found for (1). The structures were completed by a series of three-dimensional Fourier and difference-Fourier

maps, each successive map being phased by an increasing number of atoms.

The Fourier syntheses showed the existence of two different unco-ordinated Hbipyam⁺ molecules in the crystal lattice. Both are disordered around two-fold axes perpendicular to the aromatic planes and passing between the two rings. This was interpreted in terms of a statistical disorder around the axes. On the basis of this hypothesis occupancy factors of the ring atoms and the bridging nitrogen atom were fixed at 1.00 and 0.50 respectively. A series of full-matrix least-squares cycles with anisotropic thermal parameters for the metal and phosphorus atoms and isotropic thermal parameter for all the other non-hydrogen atoms were performed with SHELX 76.¹³ Owing to the low number of observed reflections rigid-group refinement was used for the pyridine rings of Hbipyam⁺. The choice between the two possible enantiomeric structures was made on the basis of the known absolute configuration of D-ribose.

Atomic scattering factors of C, N, O, and P were taken from SHELX 76¹³; those of Mg and Ca were taken from ref. 17.

Final atomic co-ordinates with estimated standard deviations are reported in Table 4; the standard deviations are somewhat large and prevent a detailed discussion of bond lengths and angles. The main source of experimental error lies in the low ratio between the number of observed intensities and the number of parameters, 4.99 and 4.75 for (1) and (2) respectively. This is most likely due to the difficulty in obtaining good crystals. Furthermore the presence of disorder in the bipyam molecules and in the molecules of water of crystallization do not allow better results. However we believe that the essential features of the structures are correct and that the molecular geometry can be confidently discussed.

The agreement index $R = \Sigma(|F_o| - |F_c|) / \Sigma|F_o|$ was 0.111 and 0.124 for (1) and (2) respectively. The index $R' = [\Sigma w(|F_o| - |F_c|)^2 / \Sigma w F_o^2]^{1/2}$ was reduced to 0.110 and 0.127 respectively. The function minimized was $\Sigma w(|F_o| - |F_c|)^2$ with weights $w = 1/[\sigma^2(F) + aF^2]$, where *a* is a variable parameter refined to 0.0580 for (1) and 0.0189 for (2).

Results and Discussion

Description of the Structures.—The elemental analyses shown in Table 1 are confirmed by the X-ray determinations of (1) and (2). Since many water molecules are only weakly linked by hydrogen bonds and can easily escape the micro-crystalline solids the results of analytical measurements depend on the storage conditions of the compounds.

On the basis of the potentiometric titration studies and from the values of the acidity constants for the protons in $\text{H}_2\text{atp}^{2-}$ ($\text{p}K_a[\text{N}(1)] = 4.06$, $\text{p}K_a(\gamma\text{-phosphate}) = 6.53$)¹⁸ and for protonated bipyam ($\text{p}K_a = 7.14$)¹⁹ it is likely that in complexes (1)–(7) (crystallized at a pH value of about 5) the γ -phosphate groups and the bipyam molecules are protonated. On the other hand the interaction between the metal ions and the triphosphate chain can increase the acidity constant of the γ -phosphate group. Therefore the N(1) nitrogen atom of the purine system is likely to be protonated. This seems to be in agreement with the results of the structure of Mn(Hatp)-(Hbipyam).⁸

Relevant bond lengths and angles around the metal atoms and in the phosphate chain for both (1) and (2) are listed in Tables 5 and 6 respectively.

The crystals of both (1) and (2) contain $[\text{M}(\text{Hatp})_2]^{4-}$ anions, $[\text{M}(\text{H}_2\text{O})_6]^{2+}$ cations, unco-ordinated Hbipyam⁺ cations, and several free water molecules. The compounds can thus be formulated as $[\text{Mg}(\text{H}_2\text{O})_6][\text{Hbipyam}]_2[\text{Mg}(\text{Hatp})_2]$.

Table 4. Atomic co-ordinates ($\times 10^4$) for the ternary complexes (1) and (2)

(a) Complex (1)				(b) Complex (2)			
Atom	X/a	Y/b	Z/c	Atom	X/a	Y/b	Z/c
Mg(1)	5 287(6)	0	0	Ca(1)	5 213(4)	0	0
Mg(2)	6 025(10)	5 000	0	Ca(2)	6 057(10)	5 000	0
P(1)	4 553(3)	1 500(7)	755(3)	P(1)	4 503(4)	1 503(17)	828(3)
P(2)	5 252(4)	-769(9)	982(3)	P(2)	5 182(4)	-828(15)	1 024(3)
P(3)	6 620(3)	816(9)	732(3)	P(3)	6 215(4)	659(14)	784(3)
O(5')	3 919(8)	1 689(21)	857(6)	O(5')	3 869(11)	1 644(30)	942(8)
O(2)	4 882(9)	2 653(20)	929(7)	O(2)	4 790(14)	2 728(37)	991(10)
O(3)	4 639(8)	1 194(20)	279(6)	O(3)	4 552(11)	1 265(32)	343(9)
O(4)	4 709(9)	203(22)	1 057(7)	O(4)	4 669(10)	138(28)	1 074(7)
O(5)	5 205(9)	-1 717(23)	1 343(7)	O(5)	5 139(12)	-1 858(32)	1 355(9)
O(6)	5 274(7)	-1 188(17)	545(6)	O(6)	5 173(10)	-1 309(26)	580(7)
O(7)	5 823(9)	117(25)	1 081(7)	O(7)	5 758(8)	-38(25)	1 101(6)
O(8)	6 784(10)	-55(29)	692(9)	O(8)	6 707(15)	-158(42)	739(10)
O(9)	5 913(8)	968(20)	330(6)	O(9)	5 915(9)	863(28)	402(7)
O(10)	6 394(9)	2 073(21)	969(7)	O(10)	6 381(12)	1 979(35)	1 002(9)
O(4')	2 971(9)	1 038(23)	1 430(7)	O(4')	2 954(10)	1 046(27)	1 498(7)
O(2')	2 618(10)	4 425(23)	1 437(8)	O(2')	2 625(13)	4 374(35)	1 535(10)
O(3')	2 025(11)	2 518(27)	926(9)	O(3')	2 006(12)	2 522(33)	1 046(9)
N(1)	3 500(11)	2 203(25)	3 246(8)	N(1)	3 533(10)	2 072(27)	3 210(7)
C(2)	2 976(11)	2 161(28)	3 056(9)	C(2)	2 986(14)	1 949(41)	3 034(11)
N(3)	2 870(9)	2 174(24)	2 632(8)	N(3)	2 866(11)	2 146(33)	2 635(9)
C(4)	3 324(12)	2 336(32)	2 379(10)	C(4)	3 379(11)	2 120(33)	2 406(9)
C(5)	3 923(12)	2 282(29)	2 533(10)	C(5)	3 912(11)	2 190(30)	2 563(8)
C(6)	3 972(12)	2 288(30)	2 991(10)				
N(1D)	5 570(6)	-1 022(26)	2 301(17)	N(1D)	5 558(7)	-1 183(28)	2 295(6)
C(1D)	5 524(6)	-986(26)	2 750(7)	C(1D)	5 523(7)	-1 136(28)	2 725(6)
C(2D)	6 031(6)	-916(26)	3 002(7)	C(2D)	6 029(7)	-1 043(28)	2 960(6)
C(3D)	6 583(6)	-883(26)	2 807(7)	C(3D)	6 571(7)	-996(28)	2 766(6)
C(4D)	6 629(6)	-919(26)	2 358(7)	C(4D)	6 606(7)	-1 044(28)	2 337(6)
C(5D)	6 122(6)	-989(26)	2 105(7)	C(5D)	6 099(7)	-1 137(28)	2 101(6)
N(2D)	4 979(11)	-1 117(39)	2 849(13)	N(2D)	4 996(20)	-1 186(53)	2 825(14)
N(6)	4 505(10)	2 332(23)	3 199(8)	C(6)	3 994(12)	2 199(32)	2 961(9)
N(7)	4 317(10)	2 427(23)	2 202(8)	N(6)	4 531(11)	2 193(32)	3 172(9)
N(9)	3 389(10)	2 392(24)	1 955(9)	N(7)	4 294(10)	2 324(28)	2 207(8)
C(8)	4 020(13)	2 574(31)	1 870(11)	N(9)	3 386(9)	2 299(26)	2 003(7)
C(1')	2 938(13)	2 187(32)	1 646(10)	C(8)	3 986(13)	2 391(34)	1 911(10)
C(2')	2 931(13)	3 208(33)	1 273(11)	C(1')	2 884(14)	2 157(40)	1 725(10)
C(3')	2 677(12)	2 509(29)	888(10)	C(2')	2 921(15)	3 187(44)	1 387(12)
C(4')	2 887(14)	1 102(33)	967(12)	C(3')	2 658(13)	2 439(40)	1 015(11)
C(5')	3 419(14)	755(38)	739(13)	C(4')	2 816(16)	1 003(45)	1 076(12)
O(W1)	6 441(16)	3 117(42)	-158(13)	C(5')	3 425(20)	513(50)	834(14)
O(W2)	5 906(23)	4 279(57)	602(17)	O(W1)	6 393(19)	2 837(54)	-168(15)
O(W3)	5 313(20)	3 804(49)	-204(14)	O(W2)	5 709(19)	3 898(49)	573(14)
O(WD1)	7 390(24)	0	0	O(W3)	5 167(29)	4 056(78)	-323(22)
O(WD2)	6 129(17)	1 823(47)	1 205(13)	O(WD1)	7 298(22)	0	0
O(WD3)	8 559(38)	0	0	O(WD2)	8 029(33)	1 713(99)	1 219(25)
O(WD4)	8 829(18)	2 640(44)	314(15)	O(WD3)	9 495(28)	638(88)	1 432(23)
O(WD5)	5 548(20)	4 900(54)	4 258(17)	O(WD4)	8 799(23)	3 004(67)	187(17)
O(WD6)	7 669(18)	3 045(45)	336(14)	O(WD5)	7 701(26)	3 132(76)	132(23)
O(WD7)	-606(29)	1 327(81)	1 379(23)				
N(1D1)	413(12)	595(46)	2 086(16)	N(1D1)	414(13)	593(47)	2 175(14)
C(1D1)	616(12)	606(46)	2 510(16)	C(1D1)	638(13)	596(47)	2 575(14)
C(2D1)	1 219(12)	627(46)	2 594(16)	C(2D1)	1 238(13)	539(47)	2 638(14)
C(3D1)	1 619(12)	637(46)	2 252(16)	C(3D1)	1 615(13)	480(47)	2 301(14)
C(4D1)	1 416(12)	626(46)	1 828(16)	C(4D1)	1 391(13)	477(47)	1 900(14)
C(5D1)	813(12)	605(46)	1 744(16)	C(5D1)	791(13)	533(47)	1 837(14)
N(2D1)	352(61)	490(172)	2 887(29)	N(2D1)	96(23)	434(128)	2 695(30)

12H₂O (1) and [Ca(H₂O)₆][Hbipyam]₂[Ca(Hatp)₂·9H₂O (2).

In the [M(Hatp)₂]⁴⁺ unit (Figure 2) the metal ion has an octahedral co-ordination geometry and is located on a two-fold axis. The two Hatp³⁻ molecules interact with the metal centre *via* the α , β , and γ phosphate oxygen atoms. The

co-ordination polyhedron of Mg(1) is nearly regular. The six Mg(1)-O bond distances average 2.06(2) Å. The co-ordination polyhedron of Ca(1) in compound (2) is a little more distorted as shown by the O-Ca(1)-O bond angles. The Ca(1)-O distances average 2.28(2) Å.

No interaction exists between the metal ions and the

Table 5. Bond lengths (Å) for complexes (1) and (2)

Complex (1)				Complex (2)			
Mg(1)—O(3)	2.10(2) × 2	N(1)—C(2)	1.33(3)	Ca(1)—O(3)	2.28(3) × 2	N(1)—C(2)	1.39(4)
Mg(1)—O(6)	2.08(2) × 2	C(2)—N(3)	1.34(4)	Ca(1)—O(6)	2.30(2) × 2	C(2)—N(3)	1.34(4)
Mg(1)—O(9)	2.01(2) × 2	N(3)—C(4)	1.31(3)	Ca(1)—O(9)	2.25(2) × 2	N(3)—C(4)	1.39(3)
		C(4)—C(5)	1.44(4)			C(4)—C(5)	1.33(4)
Mg(2)—O(W1)	2.20(4) × 2	C(5)—C(6)	1.42(4)	Ca(2)—O(W1)	2.39(5) × 2	C(5)—C(6)	1.30(4)
Mg(2)—O(W2)	2.03(5) × 2	C(6)—N(1)	1.34(4)	Ca(2)—O(W2)	2.31(5) × 2	C(6)—N(1)	1.34(3)
Mg(2)—O(W3)	2.12(5) × 2	C(6)—N(6)	1.37(3)	Ca(2)—O(W3)	2.49(7) × 2	C(6)—N(6)	1.41(4)
		C(5)—N(7)	1.37(4)			C(5)—N(7)	1.46(3)
P(1)—O(5')	1.49(2)	N(7)—C(8)	1.24(4)	P(1)—O(5')	1.50(3)	N(7)—C(8)	1.19(3)
P(1)—O(2)	1.50(2)	C(8)—N(9)	1.47(4)	P(1)—O(2)	1.50(4)	C(8)—N(9)	1.41(4)
P(1)—O(3)	1.52(2)	N(9)—C(4)	1.32(4)	P(1)—O(3)	1.59(3)	N(9)—C(4)	1.32(3)
P(1)—O(4)	1.66(2)	N(9)—C(1')	1.42(4)	P(1)—O(4)	1.64(3)	N(9)—C(1')	1.47(4)
P(2)—O(4)	1.60(2)			P(2)—O(4)	1.54(3)		
P(2)—O(5)	1.48(2)	O(4')—C(1')	1.36(4)	P(2)—O(5)	1.50(3)	O(4')—C(1')	1.35(4)
P(2)—O(6)	1.42(2)	C(1')—C(2')	1.56(5)	P(2)—O(6)	1.52(3)	C(1')—C(2')	1.51(5)
P(2)—O(7)	1.61(2)	C(2')—C(3')	1.51(4)	P(2)—O(7)	1.57(2)	C(2')—C(3')	1.55(5)
P(3)—O(7)	1.63(2)	O(2')—C(2')	1.52(4)	P(3)—O(7)	1.63(2)	O(2')—C(2')	1.46(5)
P(3)—O(8)	1.49(3)	O(3')—C(3')	1.49(4)	P(3)—O(8)	1.41(4)	O(3')—C(3')	1.50(4)
P(3)—O(9)	1.48(2)	C(3')—C(4')	1.54(4)	P(3)—O(9)	1.43(2)	C(3')—C(4')	1.51(5)
P(3)—O(10)	1.51(2)	O(4')—C(4')	1.45(4)	P(3)—O(10)	1.56(3)	O(4')—C(4')	1.40(4)
		C(4')—C(5')	1.44(5)			C(4')—C(5')	1.68(6)
		O(5')—C(5')	1.53(4)			O(5')—C(5')	1.58(5)
		N(2D)—C(1D)	1.28(3)			N(2D)—C(1D)	1.25(3)
		N(2D1)—C(1D1)	1.32(3)			N(2D1)—C(1D1)	1.31(3)

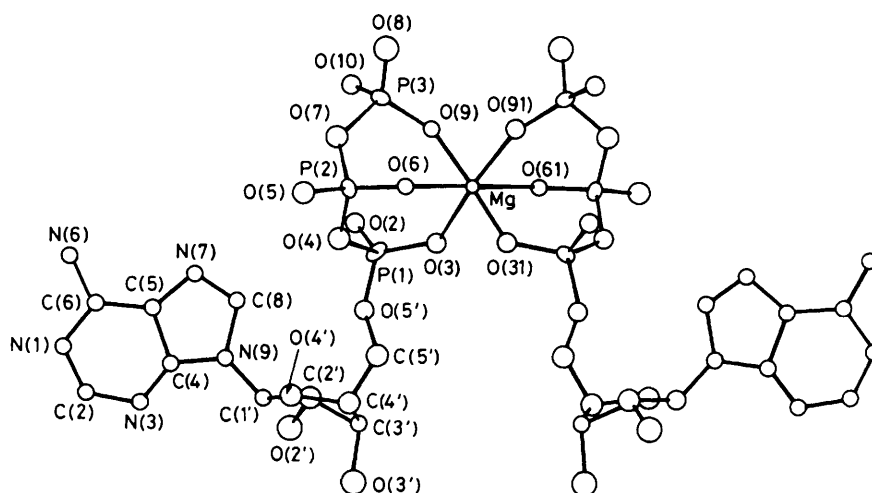


Figure 2. ORTEP drawing of the $[Mg(Hatp)_2]^{4-}$ anion in the structure of $[Mg(H_2O)_6][Hbipyam]_2[Mg(Hatp)_2] \cdot 12H_2O$ (1) The view is parallel to the b axis

nitrogen atoms of the purine system or the sugar oxygen atoms.

The M—O bond distances are a little shorter than the sum of the ionic radii. From the values of Shannon and Prewitt²⁰ the $Mg^{2+}-O^{2-}$ and $Co^{2+}-O^{2-}$ separations should be 2.12 and 2.40 Å respectively.

Most of the triphosphate chain oxygen atoms are involved in the network of hydrogen bonds with unco-ordinated water molecules, with the water molecules of the $[M(H_2O)_6]^{2+}$ cations, and with some nitrogen atoms of the adenine moiety.

The triphosphate chain. The triphosphate chain has a folded configuration in both (1) and (2). The $P(1) \cdots P(2) \cdots P(3)$ angles are $85.4(7)$ and $87.5(9)^\circ$ respectively. The folded configuration is rather common for atp complexes as shown in the structures of $Na_2(H_2atp) \cdot 3H_2O$,²¹ $\{[Zn^{II}(H_2atp)(bipy)]_2\} \cdot 4H_2O$,⁷ and $\{[Cu^{II}(H_2atp)(phen)]_2\} \cdot 7H_2O$ (phen = 1,10-phenanthroline).²²

Significant torsion angles of the present structures are reported in Table 7.

The chelate rings of the α and β phosphate groups have a chair conformation. The metal and O(4) oxygen atoms deviate $+0.71$, -0.49 and $+0.84$, -0.47 Å in (1) and (2) respectively from the plane defined by O(3), P(1), P(2), and O(6). The chelate rings of the β and γ phosphate groups have a skew-boat conformation with the P(2), O(7), P(3), O(9) atoms approximately coplanar and the metal and O(6) oxygen atoms deviating on the same side of the plane by $+0.34$, $+0.83$ and $+0.34$, $+0.87$ Å. The chelate rings involving the α and β phosphate groups are flatter than those involving the β and γ groups as shown by the values of the Q_T parameter:²³ $Q_T(\alpha, \beta) = 0.45$ and 0.50 while $Q_T(\beta, \gamma) = 0.56$ and 0.57 for (1) and (2) respectively.

The values of the triphosphate chain bond distances and angles (Tables 5 and 6) are in good agreement with the para-

Table 6. Bond angles (°) for the complexes (1) and (2)

Complex (1)				Complex (2)			
O(3)-Mg(1)-O(6)	90(1)	O(W1)-Mg(2)-O(W2)	87(2)	O(3)-Ca(1)-O(6)	84(1)	O(W1)-Ca(2)-O(W2)	81(2)
O(3)-Mg(1)-O(9)	90(1)	O(W1)-Mg(2)-O(W3)	76(2)	O(3)-Ca(1)-O(9)	89(1)	O(W1)-Ca(2)-O(W3)	79(2)
O(6)-Mg(1)-O(9)	83(1)	O(W2)-Mg(2)-O(W3)	88(2)	O(6)-Ca(1)-O(9)	77(1)	O(W2)-Ca(2)-O(W3)	82(2)
O(3)-Mg(1)-O(31)	91(1)	O(W1)-Mg(2)-O(W11)	129(2)	O(3)-Ca(1)-O(31)	96(1)	O(W1)-Ca(2)-O(W11)	142(3)
O(3)-Mg(1)-O(61)	89(1)	O(W1)-Mg(2)-O(W21)	100(2)	O(3)-Ca(1)-O(61)	93(1)	O(W1)-Ca(2)-O(W21)	112(2)
O(6)-Mg(1)-O(61)	178(1)	O(W1)-Mg(2)-O(W31)	154(2)	O(3)-Ca(1)-O(91)	168(1)	O(W1)-Ca(2)-O(W31)	136(2)
O(6)-Mg(1)-O(91)	98(1)	O(W2)-Mg(2)-O(W21)	165(2)	O(6)-Ca(1)-O(61)	175(1)	O(W2)-Ca(2)-O(W21)	140(2)
O(9)-Mg(1)-O(31)	172(1)	O(W2)-Mg(2)-O(W31)	80(2)	O(6)-Ca(1)-O(91)	106(1)	O(W2)-Ca(2)-O(W31)	64(2)
O(9)-Mg(1)-O(91)	90(1)	O(W3)-Mg(2)-O(W31)	81(2)	O(9)-Ca(1)-O(91)	88(1)	O(W3)-Ca(2)-O(W31)	70(2)
Mg-O(3)-P(1)	127(1)	P(1)-O(5')-C(5')	126(2)	Ca(1)-O(3)-P(1)	128(2)	P(1)-O(5')-C(5')	120(3)
Mg-O(6)-P(2)	127(1)	P(1)-O(4)-P(2)	125(1)	Ca(1)-O(6)-P(2)	126(2)	P(1)-O(4)-P(2)	131(2)
Mg-O(9)-P(3)	139(1)	P(2)-O(7)-P(3)	127(1)	Ca(1)-O(9)-P(3)	142(2)	P(2)-O(7)-P(3)	132(1)
O(5')-P(1)-O(2)	108(1)	O(7)-P(2)-O(4)	104(1)	O(5')-P(1)-O(2)	105(2)	O(7)-P(2)-O(4)	108(1)
O(5')-P(1)-O(3)	111(1)	O(7)-P(2)-O(5)	106(1)	O(5')-P(1)-O(3)	109(1)	O(7)-P(2)-O(5)	107(1)
O(5')-P(1)-O(4)	101(1)	O(7)-P(2)-O(6)	109(1)	O(5')-P(1)-O(4)	101(1)	O(7)-P(2)-O(6)	109(1)
O(3)-P(1)-O(2)	117(1)	O(7)-P(3)-O(8)	106(1)	O(3)-P(1)-O(2)	116(2)	O(7)-P(3)-O(8)	109(2)
O(4)-P(1)-O(2)	109(1)	O(7)-P(3)-O(9)	106(1)	O(4)-P(1)-O(2)	115(1)	O(7)-P(3)-O(9)	107(2)
O(4)-P(1)-O(3)	111(1)	O(7)-P(3)-O(10)	100(1)	O(4)-P(1)-O(3)	109(2)	O(7)-P(3)-O(10)	104(1)
O(5)-P(2)-O(4)	104(1)	O(8)-P(3)-O(9)	115(1)	O(5)-P(2)-O(4)	108(1)	O(8)-P(3)-O(9)	112(2)
O(6)-P(2)-O(4)	110(1)	O(8)-P(3)-O(10)	113(1)	O(6)-P(2)-O(4)	107(1)	O(8)-P(3)-O(10)	111(1)
O(6)-P(2)-O(5)	121(1)	O(9)-P(3)-O(10)	115(1)	O(6)-P(2)-O(5)	117(2)	O(9)-P(3)-O(10)	113(2)
N(9)-C(1')-O(4')	115(2)	O(3')-C(3')-C(2')	108(2)	N(9)-C(1')-O(4')	109(3)	O(3')-C(3')-C(2')	108(3)
N(9)-C(1')-C(4')	114(3)	O(3')-C(3')-C(4')	108(2)	N(9)-C(1')-C(2')	109(3)	O(3')-C(3')-C(4')	106(3)
C(2')-C(1')-O(4')	102(2)	C(3')-C(4')-C(5')	114(3)	C(2')-C(1')-O(4')	100(3)	C(3')-C(4')-C(5')	115(3)
C(1')-C(2')-C(3')	106(2)	C(3')-C(4')-O(4')	104(2)	C(1')-C(2')-C(3')	102(3)	C(3')-C(4')-O(4')	99(3)
C(1')-C(2')-O(2')	108(2)	C(5')-C(4')-O(4')	111(3)	C(1')-C(2')-O(2')	108(3)	C(5')-C(4')-O(4')	106(3)
C(3')-C(2')-O(2')	118(2)	C(1')-O(4')-C(4')	116(2)	C(3')-C(2')-O(2')	118(3)	C(1')-O(4')-C(4')	122(3)
C(2')-C(3')-C(4')	101(2)	O(5')-C(5')-C(4')	110(3)	C(2')-C(3')-C(4')	106(3)	O(5')-C(5')-C(4')	103(3)
C(2)-N(1)-C(6)	117(2)	N(1)-C(6)-C(5)	122(3)	C(2)-N(1)-C(6)	119(3)	N(1)-C(6)-C(5)	119(2)
N(1)-C(2)-N(3)	127(2)	N(1)-C(6)-N(6)	116(3)	N(1)-C(2)-N(3)	125(3)	N(1)-C(6)-N(6)	113(3)
C(2)-N(3)-C(4)	117(2)	C(5)-C(6)-N(6)	122(3)	C(2)-N(3)-C(4)	110(2)	C(5)-C(6)-N(6)	127(3)
N(3)-C(4)-C(5)	123(3)	C(5)-N(7)-C(8)	106(2)	N(3)-C(4)-C(5)	125(2)	C(5)-N(7)-C(8)	106(2)
N(3)-C(4)-N(9)	134(3)	N(7)-C(8)-N(9)	112(3)	N(3)-C(4)-N(9)	122(2)	N(7)-C(8)-N(9)	114(3)
C(5)-C(4)-N(9)	103(2)	C(4)-N(9)-C(8)	107(2)	C(5)-C(4)-N(9)	111(2)	C(4)-N(9)-C(8)	103(2)
C(4)-C(5)-N(6)	114(2)	C(4)-N(9)-C(1')	126(2)	C(4)-C(5)-N(6)	121(2)	C(4)-N(9)-C(1')	126(2)
C(4)-C(5)-N(7)	111(3)	C(8)-N(9)-C(1')	127(3)	C(4)-C(5)-N(7)	105(2)	C(8)-N(9)-C(1')	130(2)
C(6)-C(5)-N(7)	134(3)			C(6)-C(5)-N(7)	134(2)		

meters of the triphosphate group in $\text{Na}_5(\text{P}_3\text{O}_{10})^{24}$ and in $[\text{Co}(\text{NH}_3)_4(\text{H}_2\text{P}_3\text{O}_{10})]^{25}$. However some strain increases the P-O-P and O(4)-P(2)-O(7) angles in (1) and (2) compared to that of the $\text{P}_3\text{O}_{10}^{5-}$ ion.

It is often of importance to determine the chirality of co-ordinated nucleotides as many enzymes are able to discriminate between different stereoisomers. Recently a simple nomenclature which identifies the screw sense of co-ordination without reference to the identity of the individual atoms was suggested.²⁵ On the basis of this nomenclature the enantiomers of the tridentate Hatp^{3-} complexes (1) and (2) are designated Λ -*exo*.

Ribose rings. The ribose rings show the ²E [*'envelope'*; or C(2') *endo*]²⁶ conformation in both (1) and (2). This conformation is common for metal-nucleotide complexes. The C(2') atom deviates 0.47 and 0.52 Å from the planes defined by the atoms C(1')-O(4')-C(3')-C(4') in (1) and (2) respectively. The deviations are on the same sides of the C(5') atoms.

The torsion angle O(5')-C(5')-C(4')-C(3') amounts to 57° in (1) and 46° in (2) so that the conformation around the C(4')-C(5') exocyclic angle can be referred to as *g*⁺ (*gauche*⁺) (Table 7). The values of the glycosyl torsion angles $\chi[\text{O}(4')\text{-C}(1')\text{-N}(9)\text{-C}(4)]$ are -107° in (1) and -108° in (2) corresponding to the '*anti*' conformation.

The O(3') and O(2') oxygen atoms are involved in intermolecular hydrogen bonds.

Adenine groups. The adenine atoms are essentially coplanar in each structure. None of the potential donors [N(1), N(3), N(6), and N(7)] is involved in interactions with the metal ions. The purine systems give stacking interactions with the aromatic rings of Hbipyam⁺. The N(1), N(6), and N(7) atoms show particularly short contact distances with the atoms of the amine molecules. The bond lengths and angles in the purine moieties have normal values.

The $[\text{M}(\text{H}_2\text{O})_6]^{2+}$ cations. The $[\text{M}(\text{H}_2\text{O})_6]^{2+}$ cations have a distorted octahedral geometry as shown in Tables 5 and 6. The metal centres lie on a two-fold axis. The M(2)-O distances average 2.12(6) and 2.40(7) Å in (1) and (2) respectively. All the co-ordinated water molecules are involved in hydrogen bonding with the oxygen atoms of the triphosphate chains

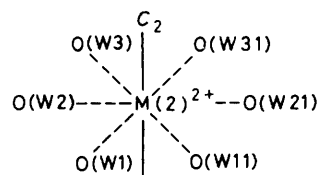
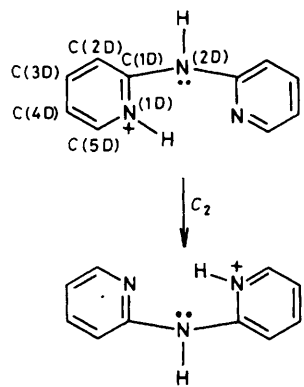


Table 7. Torsion angles ($^{\circ}$) in complexes (1) and (2)

	(1)	(2)
C(3')-C(4')...C(5')-O(5')	57	46
C(4')-C(5')...O(5')-P(1)	168	172
C(5')-O(5')...P(1)-O(2)	180	-178
C(5')-O(5')...P(1)-O(3)	51	57
C(5')-O(5')...P(1)-O(4)	-66	-58
O(5')-P(1)...O(4)-P(2)	159	162
O(2)-P(1)...O(4)-P(2)	-88	-85
O(3)-P(1)...O(4)-P(2)	41	48
P(1)-O(4)...P(2)-O(5)	178	176
P(1)-O(4)...P(2)-O(6)	-50	-57
P(1)-O(4)...P(2)-O(7)	67	60
O(4)-P(2)...O(7)-P(3)	-101	-97
O(5)-P(2)...O(7)-P(3)	150	147
O(6)-P(2)...O(7)-P(3)	17	19
P(2)-O(7)...P(3)-O(8)	-99	-102
P(2)-O(7)...P(3)-O(9)	23	20
P(2)-O(7)...P(3)-O(10)	143	140
O(4')-C(1')...N(9)-C(4)	-107	-108

**Scheme 1.**

but they do not interact with the purine nitrogen atoms. The atomic labelling in the cations is shown on p. 2472.

Bis(2-pyridyl)amine. Both complexes (1) and (2) contain two independent Hbipyam⁺ molecules. The two molecules are close to a two-fold axis and show a statistical disorder. Scheme 1 shows the protonated bipyam molecule and the two-fold axis perpendicular to the aromatic rings [the labelling in the second molecule is N(1D1), C(1D1), etc.].

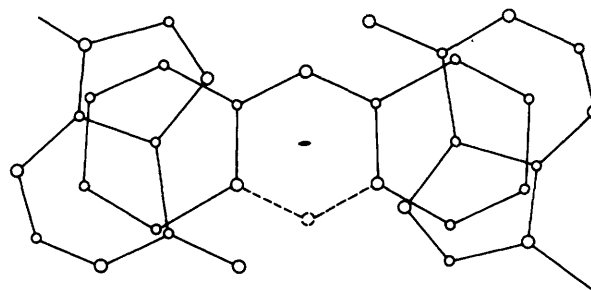
The two pyridinic rings within each Hbipyam⁺ molecule are practically coplanar. The bridging nitrogen atoms are coplanar with the rings. They are involved in hydrogen bonding with the oxygen atoms of the triphosphate chain and the water molecules. Strong and extensive bipyam-bipyam and bipyam-adenine stacking interactions exist within the crystal lattices of the two structures (see below), Figure 3.

Free water molecules. Many water molecules present in each structure are not directly bonded to the cations but are involved in the system of hydrogen bonds. Their high thermal parameters are ascribed to partial occupancy of the sites; therefore the formulae previously proposed are to be regarded as limiting formulae; the crystals are actually more or less dehydrated.

Hydrogen bonds. In Table 8 the most significant hydrogen bonds in complexes (1) and (2) are reported. All the triphosphate chain oxygen atoms except O(5'), O(4), and O(7) are involved in hydrogen bonding. The N(1) adenine nitrogen atom is involved in intermolecular hydrogen-bond formation

Table 8. Selected hydrogen bonds in complexes (1) and (2)

	(1)	(2)
O(WD1)...O(8)	2.55	2.75
O(W1)...O(9)	2.93	2.94
O(W2)...O(10)	2.76	2.85
O(W3)...O(6)	2.88	2.91
N(1)...O(10)	2.45	2.56
N(2D)...O(5)	2.61	2.76
N(7)...N(6)	2.95	2.97
O(WD7)...N(2D1)	2.50	
O(WD4)...O(3)	2.86	2.55
O(8)...O(3')	2.64	2.65
O(WD2)...O(2')	2.81	2.75
O(WD7)...O(5)	2.72	

**Figure 3.** Stacking interactions between two adenine systems and a Hbipyam⁺ molecule in the structure of (1) as viewed parallel to the *b* axis

with the O(10) oxygen atom; the N(1)...O(10) distances are 2.45 and 2.56 Å in (1) and (2) respectively. The existence of this hydrogen bond suggests the adenine is protonated at N(1). The same oxygen atom [O(10)] also forms a hydrogen bond with the O(W2) water molecule of the [M(H₂O)₆]²⁺ cation.

The O(8) atom of the γ phosphate group forms a strong hydrogen bond with the O(WD1) water molecule; O(WD1) lies on a two-fold axis and interacts with two symmetry-related O(8) atoms belonging to two Hatp³⁻ molecules bound to the same metal cation.

The ribose O(2') and O(3') atoms form hydrogen bonds with the phosphate chain oxygen atoms and with the co-ordinated and free water molecules.

The N(6) and N(7) nitrogen atoms are involved in hydrogen bonding with the N(7) and N(6) atoms of a two-fold symmetry-related adenine system. This results in two Hatp³⁻ molecules base-paired in a Hoogsteen pairing scheme.^{5b}

Stacking interactions. In Table 9 the most significant adenine-bipyam and bipyam-bipyam intermolecular contact distances are reported. The adenine-bipyam stacking interaction is shown in Figure 3. There are no adenine-adenine stacking interactions.

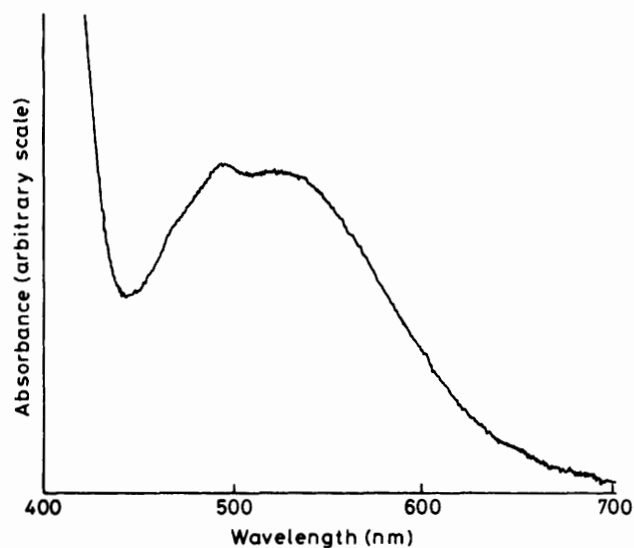
As shown in other metal-adenine nucleotide complexes the unco-ordinated N(7) atom is also involved in strong stacking interactions.^{7,27}

Infrared and Visible Spectra.—The frequencies of the absorption maxima for complexes (1)–(7) are shown in Table 10, together with data for Na₂(H₂atp) and bipyam for comparison. It appears that the antisymmetric stretching band of the α and β -PO₂⁻ groups is shifted from 1255 cm⁻¹ in Na₂(H₂atp)²⁸⁻³⁰ to \sim 1235 cm⁻¹ on complexation. As no splitting of this absorption is observed it is possible to argue that the α and β phosphates are both involved in co-ordination

Table 9. Significant stacking distances (Å) in complexes (1) and (2) *

Purine-bipyam (A)			Purine-bipyam (B), bipyam (A)-bipyam (B)			Purine-bipyam (A), bipyam (A)-bipyam (B)		
(x, y, z)	($\bar{x} + 1, y, \bar{z} - \frac{1}{2}$)	(1) M = Mg (2) M = Ca	(x, y, z)	($\bar{x} + \frac{1}{2}, y - \frac{1}{2}, \bar{z} - \frac{1}{2}$)	(1) M = Mg (2) M = Ca	(x, y, z)	($x + \frac{1}{2}, y + \frac{1}{2}, z$)	(1) M = Mg (2) M = Ca
N(1)···C(5D)		3.55 3.51	N(1)···C(3D1)		3.52 3.85	N(3)···C(3D)		3.58 3.55
C(2)···C(4D)		3.52 3.40	C(4)···C(2D1)		3.53	N(3)···C(4D)		3.53 3.56
N(3)···C(3D)		3.63 3.68	C(4)···C(3D1)		3.57 3.54	N(1D)···N(1D1)		3.54 3.31
N(3)···C(4D)		3.36 3.46	C(5)···C(1D1)		3.56 3.64	N(1D)···C(1D1)		3.51 3.40
C(4)···C(3D)		3.35 3.22	C(5)···C(2D1)		3.46 3.48	N(2D)···N(2D1)		3.58 3.47
C(4)···C(4D)		3.43 3.32	C(6)···N(1D1)		3.67 3.73	C(1D)···N(2D1)		3.65 3.62
C(5)···N(1D)		3.61 3.66	C(6)···C(4D1)		3.57 3.47	C(1D)···C(1D1)		3.57 3.36
C(5)···C(1D)		3.68 3.74	C(6)···C(5D1)		3.53 3.48	C(4D)···C(3D1)		3.54 3.53
C(5)···C(2D)		3.67 3.70	N(6)···N(1D1)		3.46 3.63	C(5D)···C(3D1)		3.66 3.88
C(5)···C(3D)		3.59 3.58	N(6)···C(5D1)		3.43 3.47	C(5D)···C(4D1)		3.63 3.56
C(5)···C(4D)		3.52 3.51	N(7)···N(2D1)		4.24 3.47			
C(5)···C(5D)		3.53 3.55	N(7)···C(1D1)		3.38 3.40			
C(6)···N(1D)		3.66 3.68	N(7)···C(2D1)		3.55 3.52			
C(6)···C(5D)		3.37 3.40	C(8)···N(2D1)		3.39			
N(7)···C(1D)		3.51 3.54	C(8)···C(2D1)		3.58 3.55			
N(7)···C(2D)		3.57 3.54	N(2D)···N(1D1)		3.49 3.40			
C(8)···C(2D)		3.59 3.51						
N(9)···C(2D)		3.63 3.65						
N(9)···C(3D)		3.43 3.43						

* bipyam (A) = C(1D)-C(5D), N(1D), N(2D); bipyam (B) = C(1D1)-C(5D1), N(1D1), N(2D1).

**Figure 4.** Reflectance spectrum of Co(Hatp)(Hbipyam) (5)

to the metal ion, as confirmed by the structural analyses of (1), (2), (4), and (5). The absorption at 910 cm^{-1} in $\text{Na}_2(\text{H}_2\text{atp})$ assigned to $-\text{P}-\text{O}-\text{P}-$ stretching vibrations²⁸⁻³⁰ is shifted to *ca.* 895 cm^{-1} in the complexes, in agreement with the presence of a triphosphate chain bound to the metal ion.

The intense absorption at 1705 cm^{-1} , attributable to the NH_2^- group deformation vibration in $\text{Na}_2(\text{H}_2\text{atp})$, shows a shift to longer wavelength (of *ca.* 15 cm^{-1}) and a splitting into two bands. No splitting is observed in the spectrum of the copper compound (6). This effect could be explained by the existence of the strong $\text{N}(1)-\text{H}\cdots\text{O}(10)$ interaction.

The i.r. spectra of complexes (1)–(7) are similar suggesting that the metal ions are also co-ordinated to the triphosphate chain of Hatp³⁻ in complexes (3), (6), and (7).

Figure 4 shows the reflectance spectrum of the cobalt complex (5). The absorptions at 490 and 525 nm can be

attributed to $d-d$ transitions of a d^7 ion in an octahedral field.⁶ A similar absorption pattern is found in neutral or weakly acidic solutions of (5).

Conclusions

This work has given important information concerning (a) the nature of the divalent metal ion-atp interactions and (b) the influence of weak linkages, like hydrogen bonds and stacking interactions, on the stability of the metal-nucleotide complexes in the solid state.

The crystal and molecular structures of complexes (1) and (2) show that in the solid state the alkaline-earth metal cations have an affinity towards the α , β , and γ phosphate group oxygen atoms. All the metal-oxygen interactions are comparable although some previous investigations suggested the $\text{M}-\text{O}_\alpha$ interaction should be weaker than the $\text{M}-\text{O}_\beta$ and $\text{M}-\text{O}_\gamma$ bonds.³¹

No interaction exists between the metal and the nitrogen atoms of the adenine system although N(7) often acts as a donor in many nucleoside or nucleotide complexes containing purine bases.³² On the other hand in metal-nucleotide-aromatic base ternary complexes the N(7) co-ordination does not take place as the metal is bound to the phosphate chain and to the second ligand.^{7,22} The metal ion-aromatic base interaction was believed to be an essential step to exclude N(7) from the co-ordination polyhedron.

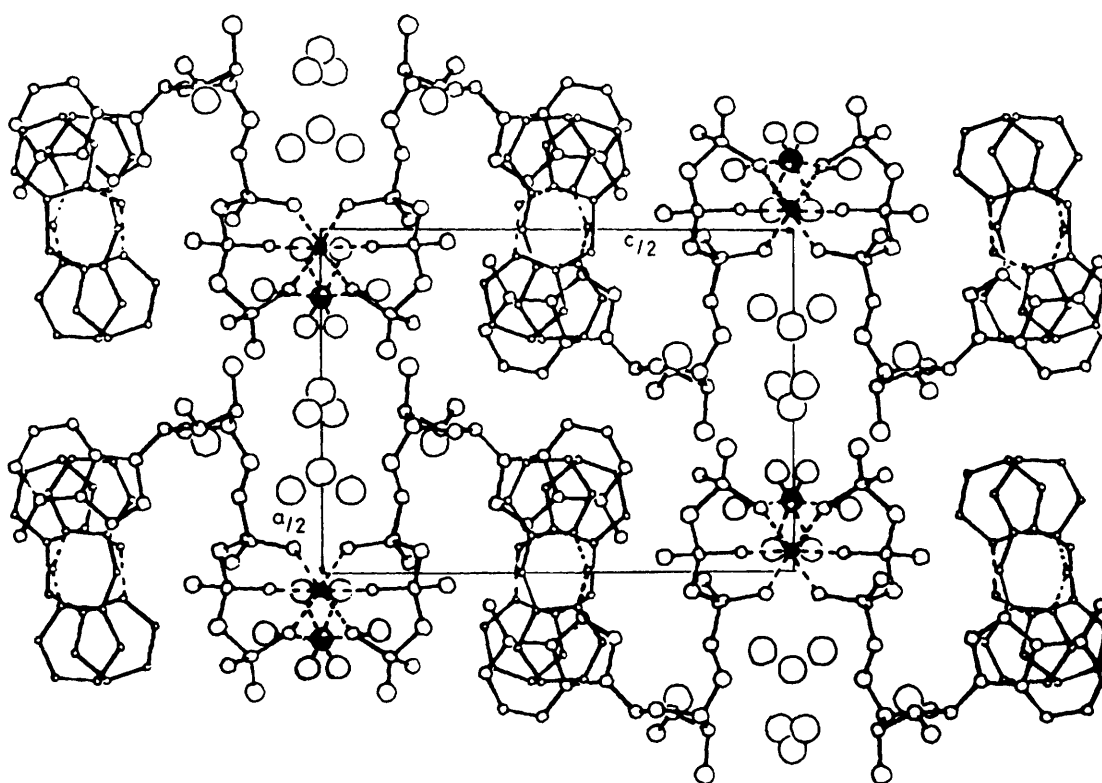
The present structures show that the metal ion can interact just with the triphosphate chain without any bond formation with either the adenine or the base nitrogen atoms.

This investigation also confirms the fundamental importance of the stacking interactions between aromatic rings in compounds of biological significance (see Figures 3 and 5).

It is evident that (1) and (2) contain hydrophilic and hydrophobic regions. The hydrophilic zones contain the ribose ring, the triphosphate chain, the metal ion (M^{2+}), and the $[\text{M}(\text{H}_2\text{O})_6]^{2+}$ cation. Extensive channels are filled by many water molecules. The hydrophobic zones are constituted by the adenine system and Hbipyam⁺ molecules. Figure 5 suggests

Table 10. I.r. absorption maxima (cm^{-1}) of bipyam, $\text{Na}_2(\text{H}_2\text{atp})$, and of the ternary complexes $\text{M}(\text{Hatp})(\text{Hbipyam}) \cdot x\text{H}_2\text{O}$ (1)–(7) in Nujol mulls in the region $1800\text{--}600\text{ cm}^{-1}$; sh = shoulder, s = strong, m = medium, w = weak

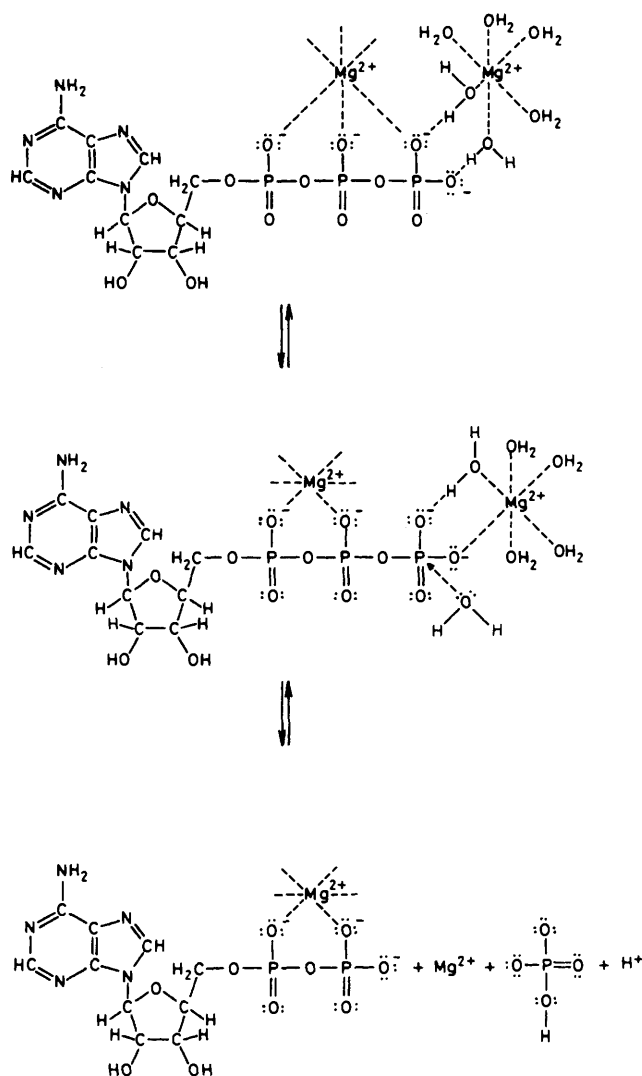
(1; M = Mg)	(2; M = Ca)	(3; M = Sr)	(4; M = Mn)	(5; M = Co)	(6; M = Cu)	(7; M = Zn)	$\text{Na}_2(\text{H}_2\text{atp})$	bipyam
1 690 (sh)	1 690 (sh)	1 690 (sh)	1 695m	1 680m	1 690s	1 690 (sh)	1 705s	
1 660s	1 660s	1 660s	1 660s	1 655s	1 640s	1 660s		1 600s
1 600s	1 600s	1 600s	1 600s	1 600s	1 585m	1 600s		1 560m
1 560s	1 560s	1 560s	1 560s	1 560s		1 560s		1 525s
								1 310m
1 245s	1 235s	1 230s	1 230s	1 230s	1 230s	1 240s	1 255s	1 145m
1 120s	1 110s	1 120s	1 120m	1 110s	1 120s	1 120s	1 110s	
1 080s	1 080s	1 080s	1 080s	1 070s	1 080s	1 080s	1 065s	
1 000m	1 000m	1 000m	1 000m	1 000m	1 000m	1 000m	1 030m	
				970m			980s	985w
895m	895m	895m	895m	895m	895s	895m	910s	
820w	820w	820w	820w	820w	820w	820m	815m	
770m	770m	770m	770m	760m	760m	770m	725m	765s
720m	720m	720m	715m	720m	715m	720m	705m	730w
							640m	

**Figure 5.** A diagram to show the existence of the hydrophilic and hydrophobic zones and the extensive stacking interactions between the purine and Hbipyam^+ systems in complex (1)

that groups like $[\text{M}(\text{Hatp})_2]^{4-}$ found in the present structures could exist in enzymatic systems. Strong π -interactions like those between the purine and the Hbipyam^+ units could link $[\text{Mg}(\text{Hatp})_2]^{4-}$ or $[\text{Ca}(\text{Hatp})_2]^{4-}$ to the aromatic moieties of the proteins. However it must be pointed out that on the basis of our results in the solid state it is impossible to establish if the $[\text{Mg}(\text{Hatp})_2]^{4-}$ and $[\text{Ca}(\text{Hatp})_2]^{4-}$ units exist in neutral aqueous solution under physiological conditions. We emphasize that the crystals were obtained from almost neutral aqueous solutions and that the lattices of all the species contain a relatively large number of water molecules.

Our complexes can be considered as interesting models to

draw some mechanisms of atp phosphoryl transfer in biological systems. Sigel³³ suggested a transfer mechanism in which the breakage of the triphosphate chain at the β, γ bridge is promoted by a $\text{M}(\alpha, \beta)\text{--M}'(\gamma)$ co-ordination system. In this hypothesis a divalent metal ion is bound to the α and β phosphate groups of an atp molecule and a second metal cation links the γ phosphate oxygen atom. Our results show that the $[\text{M}(\text{H}_2\text{O})_6]^{2+}$ cations form strong hydrogen bonds with the γ phosphate oxygen atoms and this could be considered the first step in the phosphoryl transfer (see Scheme 2). The final step could be the shift of the first metal cation from a (α, β, γ) -tridentate to a (α, β) -bidentate co-ordination site followed by direct binding of the $[\text{M}(\text{H}_2\text{O})_6]^{2+}$ cation to the γ group. At



Scheme 2.

this stage a water molecule can attack the complex generating a metal-ATP complex with (α,β)-bidentate co-ordination and HPO_4^{2-} .

Acknowledgements

We wish to thank Mrs. G. Montomoli and Mr. V. Bindi for technical assistance.

References

- 1 M. Dixon and E. Webb, *Enzyme*, 1964, **1**, 1.
- 2 W. Cleland, *Annu. Rev. Biochem.*, 1977, **36**, 77.

- 3 B. Rosenberg, 'Nucleic Acid-Metal Ion Interactions,' ed. T. G. Spiro, Wiley, New York, 1980.
- 4 R. B. Martin and Y. H. Mariam, 'Metal Ions in Biological Systems,' ed. H. Sigel, Dekker, Basel, 1980, vol. 8.
- 5 (a) L. G. Marzilli, T. J. Kistenmaker, and G. L. Eichhorn, 'Nucleic Acid-Metal Ion Interactions,' ed. T. G. Spiro, Wiley, New York, 1980, ch. 5; (b) J. K. Barton and S. J. Lippard, *ibid.*, ch. 2.
- 6 R. Cini and P. Orioli, *J. Inorg. Biochem.*, 1981, **14**, 95.
- 7 P. Orioli, R. Cini, D. Donati, and S. Mangani, *J. Am. Chem. Soc.*, 1981, **103**, 4446.
- 8 M. Sabat, R. Cini, and M. Sundaralingam, unpublished work.
- 9 R. Cini, A. Cinquantini, M. C. Burla, A. Nunzi, G. Polidori, and P. F. Zanazzi, *Chim. Ind. (Milan)*, 1982, **64**, 826.
- 10 R. Cini, M. Sabat, M. Sundaralingam, M. C. Burla, A. Nunzi, G. Polidori, and P. F. Zanazzi, *Inorg. Chim. Acta, Bioinorg. Chem.*, 1983, **79** (B7), 253; Abstracts of the 1st ICBIC, Florence, Italy, June 13-17, 1983.
- 11 R. Cini, M. Sabat, M. Sundaralingam, M. C. Burla, A. Nunzi, G. Polidori, and P. F. Zanazzi, *J. Biomol. Struct. Dyn.*, 1983, **1**, 633.
- 12 P. Main, 'A System of Computer Programs for the Automatic Solution of Crystal Structures from X-Ray Diffraction Data,' University of York, 1980.
- 13 G. M. Sheldrick, SHELX 76, program for crystal structure determination, Cambridge University, 1976.
- 14 C. Giacovazzo, *Acta Crystallogr., Sect. A*, 1977, **33**, 933.
- 15 M. C. Burla, A. Nunzi, C. Giacovazzo, and G. Polidori, *Acta Crystallogr. Sect. A*, 1981, **37**, 677.
- 16 G. L. Cascarano, C. Giacovazzo, G. Polidori, R. Spagna, and D. Viterbo, *Acta Crystallogr., Sect. A*, 1982, **38**, 663.
- 17 'International Tables for X-Ray Crystallography,' Kynoch Press, Birmingham, 1974, vol. 4.
- 18 M. M. Taqui Khan and A. E. Martell, *J. Phys. Chem.*, 1962, **66**, 10.
- 19 G. Anderegg, *Helv. Chim. Acta*, 1971, **54**, 509.
- 20 A. Shannon and C. T. Prewitt, *Acta Crystallogr., Sect. B*, 1969, **25**, 925.
- 21 O. Kennard, N. W. Isaacs, W. D. S. Motherwell, J. C. Coppola, D. L. Wampler, A. C. Larson, and D. G. Watson, *Proc. R. Soc. London, Ser. A*, 1971, **325**, 401.
- 22 W. S. Sheldrick, *Z. Naturforsch., Teil B*, 1982, **37**, 863.
- 23 D. Cremer and J. A. Pople, *J. Am. Chem. Soc.*, 1975, **97**, 1354.
- 24 A. F. Wells, 'Structural Inorganic Chemistry,' Clarendon, Oxford, 1975.
- 25 E. A. Merritt, M. Sundaralingam, R. D. Cornelius, and W. Cleland, *Biochemistry*, 1978, **17**, 3274.
- 26 IUPAC-IUB Joint Commission on Biochemical Nomenclature, *Eur. J. Biochem.*, 1983, **131**, 9.
- 27 K. Aoki, *J. Am. Chem. Soc.*, 1978, **100**, 7106.
- 28 A. Epp, T. Ramasarma, and T. R. Wetter, *Anal. Chem.*, 1954, **26**, 1649.
- 29 H. Brintzinger, *Biochim. Biophys. Acta*, 1963, **77**, 343.
- 30 F. L. Khalil and T. L. Brown, *J. Am. Chem. Soc.*, 1964, **86**, 5113.
- 31 S. L. Huang and M. D. Tsai, *Biochemistry*, 1982, **21**, 951.
- 32 R. W. Gellert and R. Bau, 'Metal Ions in Biological Systems,' ed. H. Sigel, Dekker, Basel, 1979, vol. 8.
- 33 H. Sigel, *Pure Appl. Chem.*, 1983, **55**, 137.

Received 29th November 1983; Paper 3/2122